27
5-20-81
24 to NTIS

(1)

SAND80-2372
Unlimited Release
UC-45

R4515

MASTER

Study of Factors Which Influence the Shock-Initiation Sensitivity of Hexanitrostilbene (HNS)

Alfred C. Schwarz

Prepared by Sandia National Laboratories, Albuquerque, New Mexico 87185 and Livermore, California 94550 for the United States Department of Energy under Contract DE-AC04-76DP00789

Printed March 1981

Sandia National Laboratories

SF 2900-Q(3-80)

DISTRIBUTION OF THIS DOCUMENT IS UNLIMITED

DISCLAIMER

Issued by Sandia National Laboratories, operated for the United States Department of Energy by Sandia Corporation.

Printed in the United States of America
Available from
National Technical Information Service
U. S. Department of Commerce
5285 Port Royal Road
Springfield, VA 22161

NTIS price codes
Printed copy: $5.00
Microfiche copy: A01

PAGES 1 to 2

WERE INTENTIONALLY

LEFT BLANK

SAND80-2372
Unlimited Release
Printed March 1981

Distribution Category
UC-45

Study of Factors Which Influence the Shock-Initiation Sensitivity of Hexanitrostilbene (HNS)

Alfred C. Schwarz
Initiating and Pyrotechnic Components Division 2515
Sandia National Laboratories
Albuquerque, NM 87185

Abstract

An experimental program was conducted to study factors which influence the shock initiation sensitivity of hexanitrostilbene (HNS). The six factors evaluated were: (1) powder morphology, (2) sample density, (3) test temperature, (4) sample length, (5) diameter of the impacting flyer, and (6) duration of the input stimulus. In addition, the effect of pressure duration, τ, was assessed on the initiation sensitivity of an extrudable explosive (LX-13) and of hexanitroazobenzene (HNAB) for comparison with that of superfine hexanitrostilbene (HNS-SF). The impact stimulus was provided by a polyimide flyer 1.57mm in diameter propelled by an electrically excited bursting foil. Flyer velocity determined impact pressure, P (3 to 20 GPa), and flyer thickness the shock duration, τ (0.010 to 0.150 μs), the pulse shape being rectangular.

Powder morphology was the most significant factor to influence the initiation sensitivity of HNS; with 0.035-μs pulses the smallest particle-sized HNS had a threshold pressure for initiation which was 50% of that required for the coarser HNS-II. Other factors which lowered the threshold pressure were: lower sample density, elevated test temperature, and larger diameter flyers.

HNS-SF showed a shorter growth-to-detonation distance (GTDD) than HNS-I; the GTDD was 0.56 mm at an impact pressure of 7.3 GPa.

Pulse duration affected the threshold pressure with each explosive behaving in its own characteristic manner; a P-τ characterization is essential, therefore, for all explosives of interest and should include values of τ which are equivalent to pulse durations expected in service.

Acknowledgment

Several associates contributed significantly toward providing the information contained herein. M. R. Kopczewski, Division 2515, prepared many of the test specimens and performed some of the experiments. The considerable assistance of G. J. Janser and W. H. Countryman of Division 2514 is gratefully acknowledged.

Contents

Illustrations

Figure

Tables

Tables (cont)

Study of Factors Which Influence the Shock-Initiation Sensitivity of Hexanitrostilbene (HNS)

Introduction

The use of hexanitrostilbene (HNS) in explosive components has been demonstrated[1,2] and many current applications exist. During the past several years, initiation studies have been performed on HNS in which flying plates provided the input stimuli. The following effects on initiation sensitivity have been studied:

- Explosive powder morphology
- Sample density
- Test temperature
- Sample length
- Flyer diameter
- Pulse duration.

Finally, the sensitivity of HNS has been compared to that of LX-13 (80/20 composition of PETN*/silicone rubber) and to that of hexanitroazobenzene (HNAB).

It is the purpose of this report to summarize these findings.

Experimental Technique

Test Device

The impact of a thin flying plate on an explosive provides a reproducible means for applying a pressure whose amplitude and duration can be independently controlled.

A small test device, identified as the modified TC817 and shown in Figure 1, was used to provide the input shock stimulus. The firing set is a capacitor discharge unit which, when discharged, applies a current pulse through the copper bridge foil; the vaporized foil propels the polyimide (Kapton†) flyer to the desired impact velocity. By regulating the burst current density through the bridge foil (by varying the fireset charging voltage), one can achieve various flyer velocities.

The calibration curves presented in Figure 2 resulted from VISAR** measurements of flyer velocity. The dotted line is a calibration for a smaller flyer (1.02-mm dia) with a shorter (0.38-mm) barrel. The impact pressure is controlled by flyer velocity and the duration of the pressure pulse is a function of the flyer thickness. The standard flyer thickness was 0.076 mm, but the thickness of the Kapton flyer could be varied from 0.025 to 0.25 mm (0.001 to 0.010 in.) to provide a range of pulse durations from about 0.01 to 0.15 μs. Since the shock impedance of the flyer is less than that of the explosive, a well-controlled, single-step, rectangular pulse is introduced into the test explosive. The typical pulse duration is 0.035 μs with the standard flyer.

Figure 3 illustrates the manner in which pressure and duration are determined; the solution may be obtained graphically or analytically. The Hugoniot curves for all the materials are contained in the Appendix. A single Hugoniot was assumed for all the types of HNS evaluated.

*Pentaerythritol tetranitrate

†DuPont Trademark

**Velocity Interferometer System for Any Reflector. L. M. Barker and R. E. Hollenbach, J. Appl. Phys., 43, p. 4669, 1974

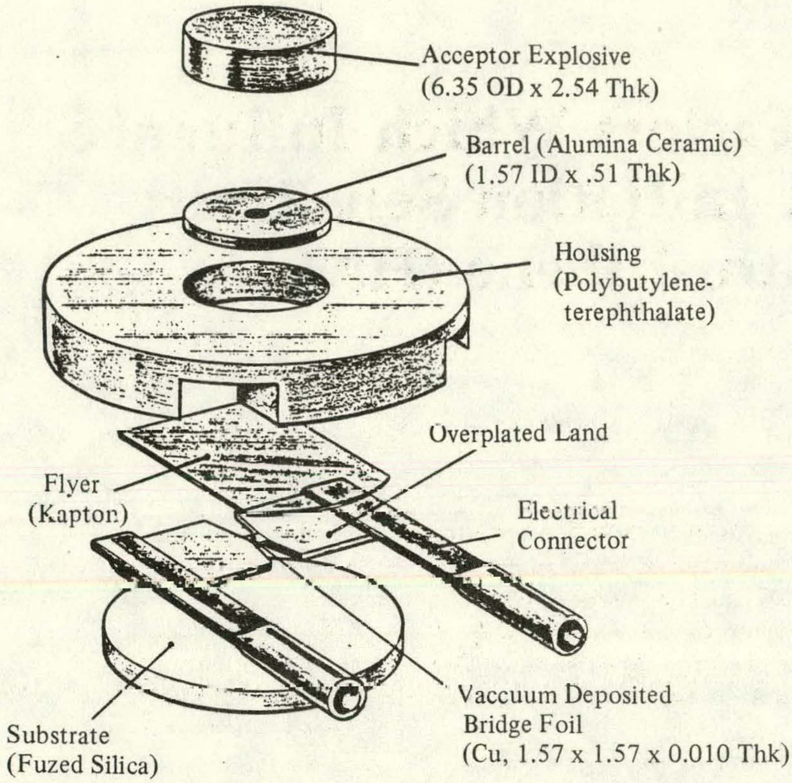

Figure 1. Modified TC817 Flying Plate Test Device (all dimensions in millimetres)

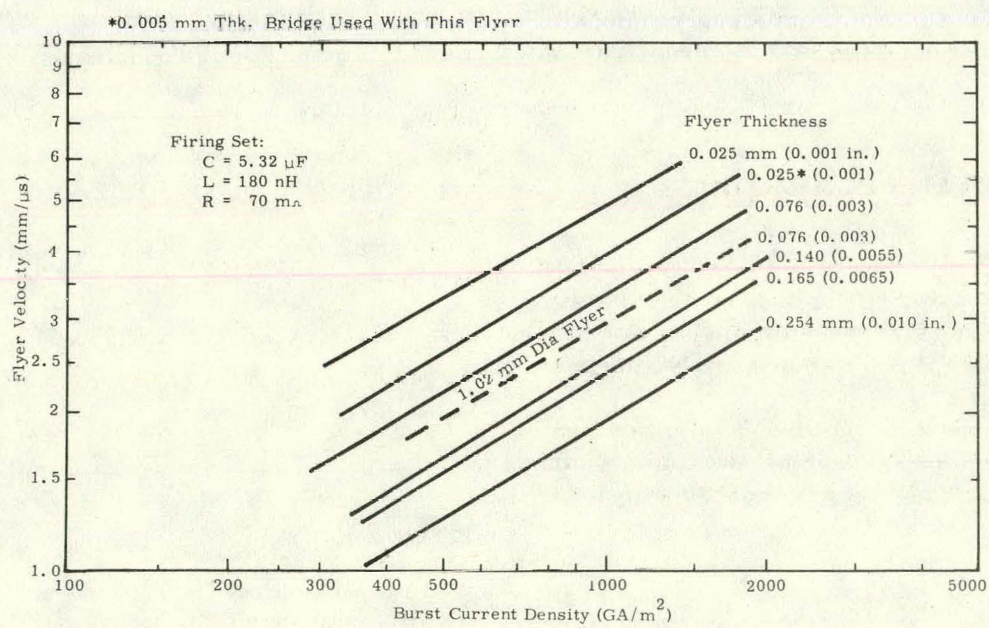

Figure 2. Flyer Velocity vs Burst Current Density (modified TC817, 1.57-mm dia flyer)

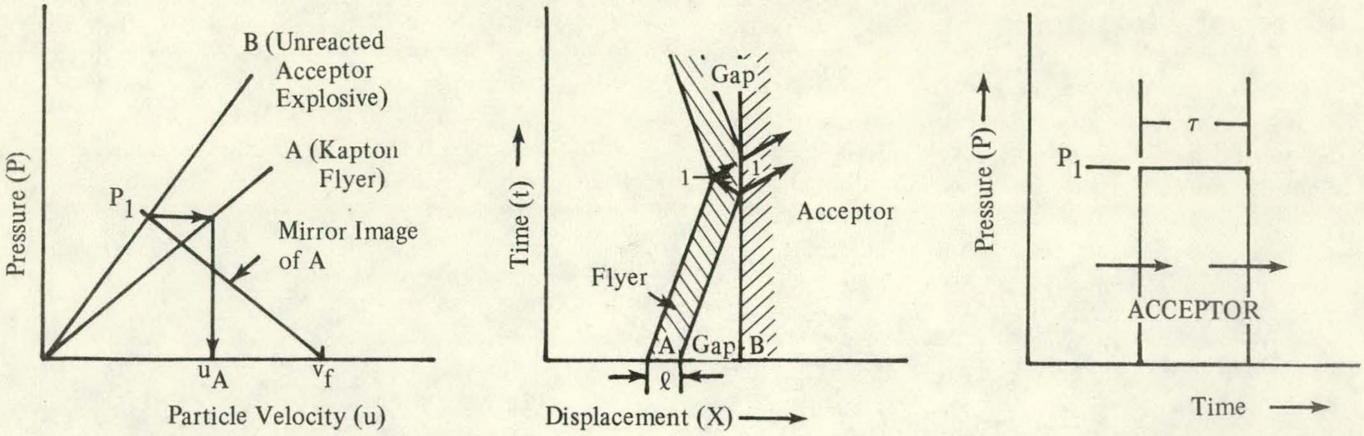

P_1 = Pressure imparted to acceptor when kapton impacts at velocity, v_f

$$\tau \cong \frac{2\ell u_A \rho_A}{P_1}$$

where

τ = pulse duration of P_1
ℓ = thickness of flyer
u_A = particle velocity in flyer
ρ_A = original density of flyer

Figure 3. Graphical Solution to Determine P_1 and τ From P-u and x-t Diagrams

Test Procedure

The explosive specimens were evaluated using the test assembly shown in Figure 4 with a free-standing test sample of the desired density, 6.35 mm in diameter and 2.54 mm long. The fire set charging voltage was preselected to provide enough flyer velocity to approximate the threshold of detonation. From this voltage level, an up-down method was used to expend the remaining test units; the charging voltage was adjusted upward after a failure to detonate and downward after a detonation. The increment of voltage used in this up-down sequence was also preselected, being larger at the outset of the testing. In each case, 24 test specimens were evaluated to provide statistical meaning to the resulting data. From the recorded voltage and current waveforms, bridge-foil current density (at burst) was determined and used as the input stimulus for the ASENT (an Analysis of Sensitivity Tests) computer program.[3] ASENT provides a calculation of the mean, standard deviation, 0.1% probability of detonation, 99.9% probability of detonation, and other applicable statistics all based on the assumption of a normal distribution. Other details of the test procedure are contained in Reference 4.

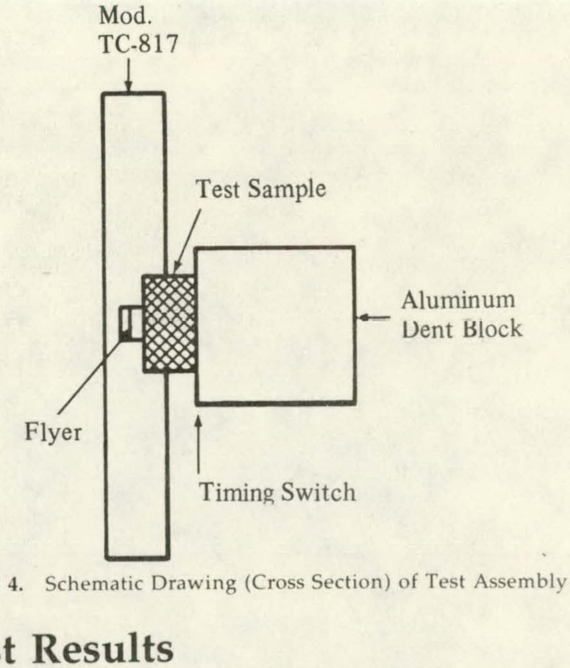

Figure 4. Schematic Drawing (Cross Section) of Test Assembly

Test Results

The sensitivity test results are divided into two groups--those earlier tests which used a 1.02-mm dia flyer and more recent tests with a 1.57-mm dia flyer. Subsequent paragraphs in which one or the other diameter was used are identified as [1] or [2], respectively.

Effect of Morphology[1]

Three types of HNS were evaluated in this series of tests--each type of explosive being made by a different process as given in Table 1. HNS-SF is a formulation (from the Teledyne Company) which has finer particles than HNS-I and very high purity. Resultant differences in morphology are illustrated in the photomicrographs in Figure 5. The Hugoniot curves for the HNS and the Kapton which were used in the determination of impact pressure are given in the Appendix.

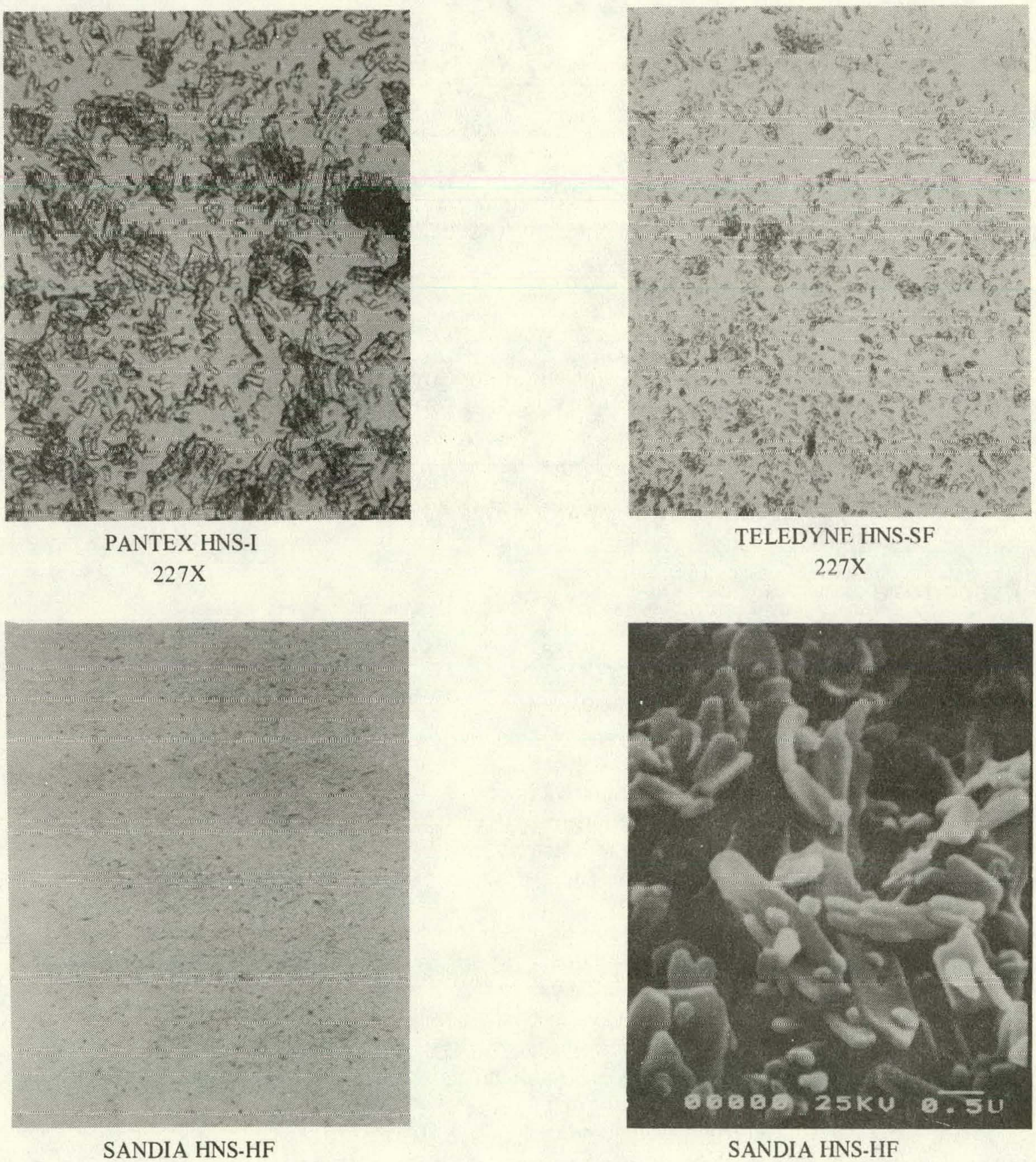

PANTEX HNS-I
227X

TELEDYNE HNS-SF
227X

SANDIA HNS-HF
500X

SANDIA HNS-HF
20000X

Figure 5. Photomicrographs of HNS Illustrating Differences in Morphology

Table 1. Comparison of Three HNS Manufacturing Processes

Process	Type	Lot	Melting Point (°C)	Surface Area (m^2/g)
Multiple Wash (Pantex)	I	7157	316-317	1.59
DMF Solution into Steam (Teledyne)	SF	-	320-321	2.56
DMF Solution into Ice H_2O (Sandia)	HF	21-28-3	319-321	>10.0

The test results are summarized in Table 2 and a probability-of-detonation plot is presented in Figure 6. This latter plot clearly illustrates the role of morphology on sensitivity; not only is the hyperfine material more sensitive but there is also a more narrow band of pressure separating detonation from nondetonation. If one adds the limited data on LX-15 (95/5 composition of HNS-I and Kel-F) and HNS-II (coarse material, specific surface area 0.4 m^2/g), the role of morphology is even more dramatic.

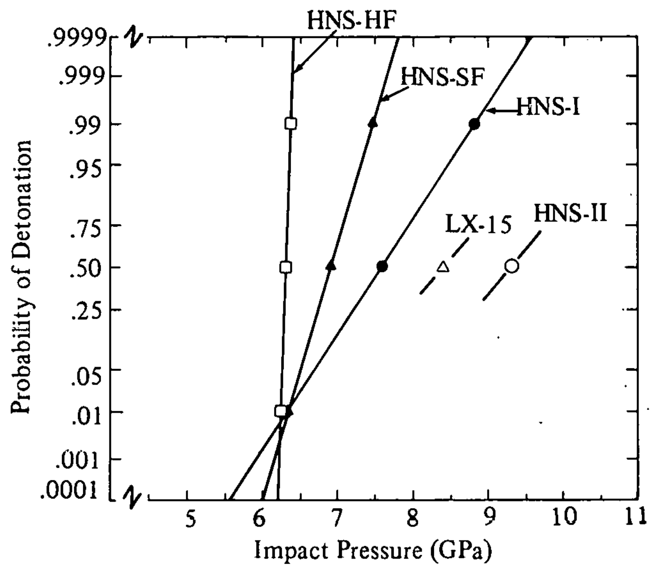

Figure 6. Effect of Morphology on Shock Initiation of HNS

Short duration pulses comparable to those of the flying plate detonator occur in applications where transfer-line end-tips or detonator end-tips are propelled across an air gap to initiate detonation. In these cases, the choice of explosive type may be guided by these results, which favor the finer particles.

However, it should be noted that the sensitivity is affected by shock duration. (See the latter sections of this report which deal with this parameter.)

Effect of Density [2]

Experiments were performed on HNS-SF at average densities of 1.30 and 1.60 Mg/m^3. Results of these tests are summarized in Table 3 and Figure 7. The initiation sensitivity was lower for the lower density specimens.

This was expected. If the explosive is treated as a porous or a distended material,[5] the absorbed energy (for internal heating) is greater for the material with greater voids (or lower density). Therefore, equivalent energy will be absorbed at a lower impact pressure for the material with the lower density.

Table 2. Summary of Shock Sensitivity Data of Three Types of HNS (1.02-mm diameter x 0.076-mm thick flyer)

Explosive	Density (Mg/m^3)	Test Temp (°C)	Initiation Threshold* J_B(GA/m^2)	v_f($mm/\mu s$)	P(GPa)	τ(μs)
HNS-I (Pantex 7157)	1.60 ±0.01	24	722 ±59	2.37	7.6	0.034
HNS-SF (Teledyne)	1.61 ±0.01	24	643 ±24	2.23	6.9	0.034
HNS-HF (SNLA, 21-28-3)	1.60 ±0.01	24	567 ± 9	2.07	6.3	0.036

*Initiation threshold is that input stimulus which produces a 50% probability of initiation to detonation. J_B is current density through the foil at burst; v_f is flyer velocity at impact with the explosive; P is the impact pressure; and τ is the pressure duration. The plus and minus values (J_B) are one standard deviation.

Table 3. Summary of Shock Sensitivity Data of HNS-SF at Two Densities (1.57-mm diameter x 0.076-mm thick flyer)

Density (Mg/m^3)	Test Temp (°C)	Initiation Threshold* J_B(GA/m^2)	v_f($mm/\mu s$)	P(GPa)	τ(μs)
1.60±0.01	24	385±16	1.84	5.3	0.038
1.30±0.01	24	350± 8	1.75	3.8	0.041**

*Initiation threshold is that input stimulus which produces a 50% probability of initiation to detonation. J_B is current density through the foil at burst; v_f is flyer velocity at impact with the explosive; P is the impact pressure; and τ is the pressure duration. The plus and minus values (J_B) are one standard deviation.

**First double transit only—subsequent staircase tail not included. Only 18 samples used in this experiment.

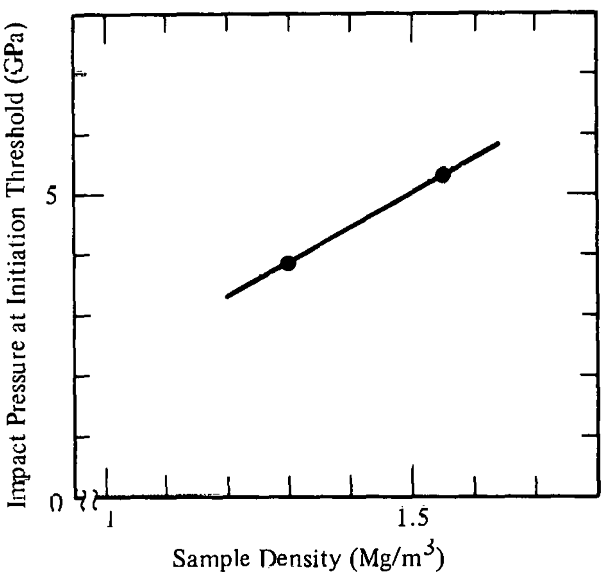

Figure 7. Effect of Sample Density on Initiation Threshold of HNS-SF

Effect of Test Temperature [1]

Experiments were performed with test specimens stabilized at each of three temperatures: +100°, +24°, and -61°C. The data from these experiments are summarized in Table 4 and in Figure 8 and are subject to two assumptions, namely: (1) the flyer velocity calibration performed at 24°C was valid for all test temperatures, and (2) the room-temperature Hugoniot properties* of the unreacted HNS were applicable to all test temperatures. The temperature

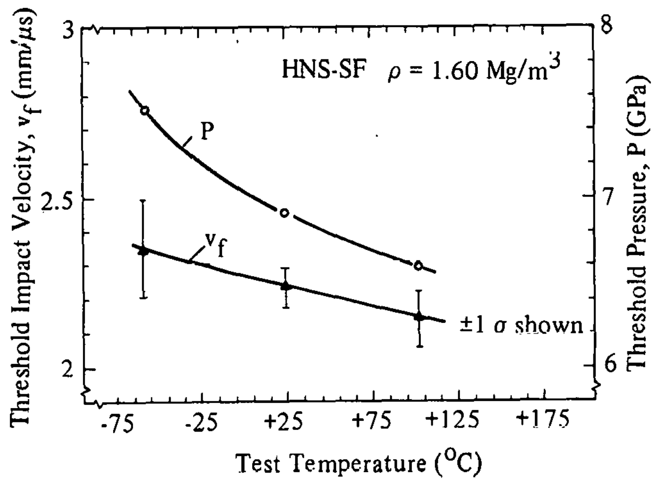

Figure 8. Effect of Temperature on Sensitivity

response appears reasonable in that one would expect less input stimulus to be required at high temperature. Other experimenters have generated confirming results.[6]

Effect of Sample Length [1]

Sample length plays an important role in the initiation process in that the length must be great enough to allow sufficient time for growth to detonation to occur.

In 1965 it was shown that a relationship existed between growth-to-detonation distances (GTDD) and applied shock pressures in polycrystalline explosives.[7] It was found that, over a wide range, the log of the run distance to detonation was linearly related to the log of the pressure of the initiating shock wave as it entered the explosive. Typical data [8] are shown in Figure 9. These data were obtained from "wedge" tests, using optical measurement techniques as indicated in Figure 10. This technique has been used by

*In Reference 6, Roth showed that their P-μ Hugoniot indicated HNS to be "softer" at high temperature; that is, the impedance at high temperature was less than at room temperature of any given pressure up to 5.0 GPa.

many experimenters for a number of years. One characteristic of note is that the input pulse duration is relatively long, for the most part being longer than the time to detonation.

The present tests had the length of the test specimen as the controlled variable. These were in four groups: 2.54, 1.27, 1.04, and 0.78 mm. The testing method was as previously described; in addition, transit time measurements were made on experiments in which samples detonated.

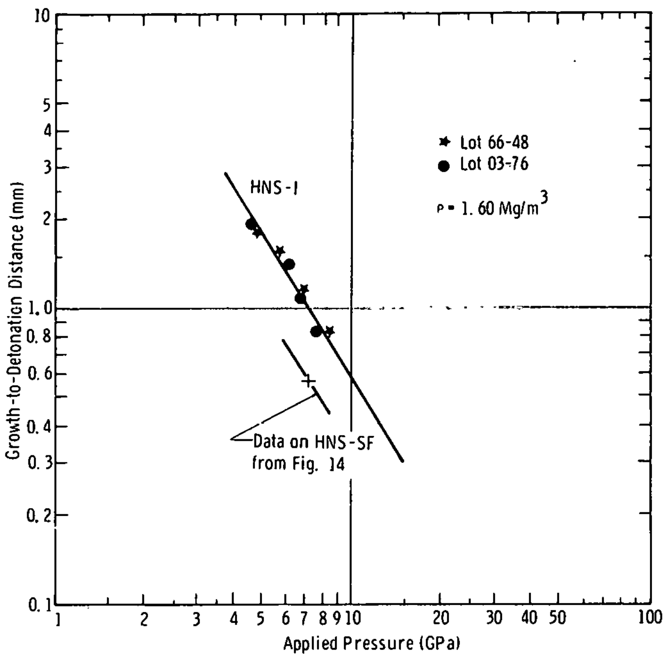

Figure 9. Wedge Test Data on HNS-I

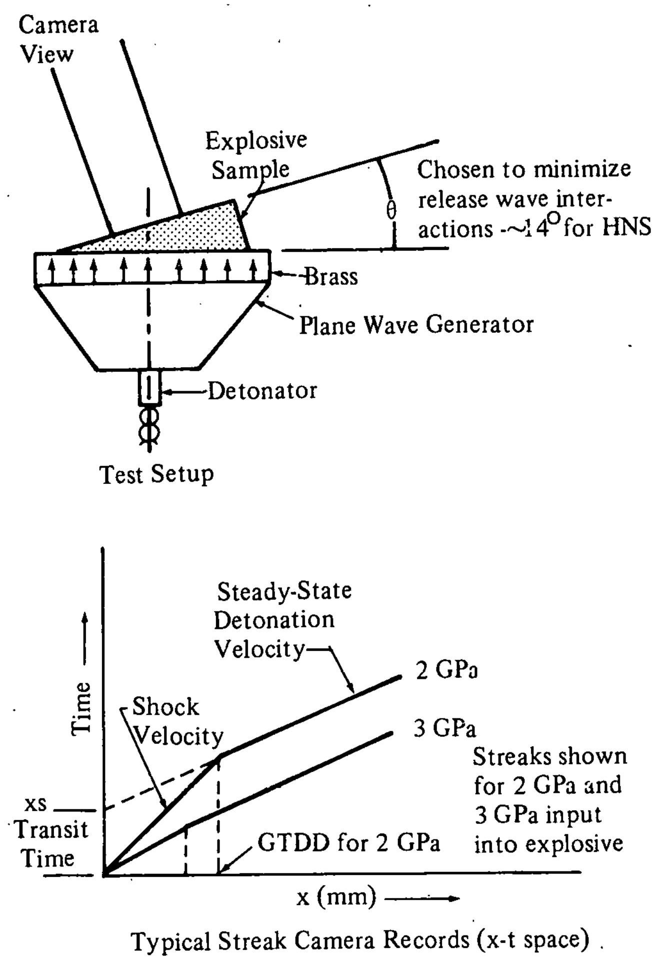

Figure 10. Wedge Test Technique

Table 4. Summary of Shock Sensitivity Data of HNS-SF as a Function of Test Temperature (1.02-mm diameter x 0.076-mm thick flyer)

Density (Mg/m^3)	Test Temp (°C)	Initiation Threshold* $J_B(GA/m^2)$	$v_f(mm/\mu s)$	P(GPa)	$\tau(\mu s)$
1.61 ± 0.01	+100	605 ± 45	2.15 ± 0.09	6.6	0.035
	+ 24	643 ± 24	2.23 ± 0.06	6.9	0.034
	− 61	707 ± 71	2.35 ± 0.14	7.5	0.034

*Initiation threshold is that input stimulus which produces a 50% probability of initiation to detonation. J_B is current density through the foil at burst; v_f is flyer velocity at impact with the explosive; P is the impact pressure; and τ is the pressure duration. The plus and minus values (J_B, v_f) are one standard deviation.

A sketch which shows the interrelationships between the shock (U_s) and the release (U_r) waves, the specimen lengths, and the predicted GTDD is shown in the P-x diagram of Figure 11. Note that the predicted GTDD at 7.3 GPa from wedge data falls at the outside of the specimen length for the shortest sample; this implies that this sample should not achieve detonation--but it did.

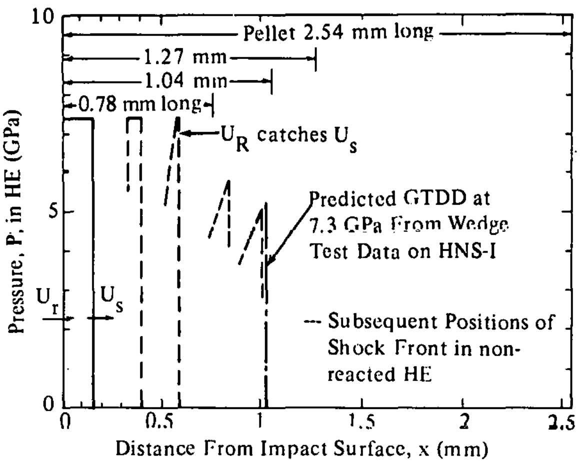

ASSUMED CONDITIONS

P = 7.3 GPa τ = 0.035 μs (rectangular)
Avg. Explosive Density = 1.58 Mg/m³
U_s = 4.00 mm/μs
U_r = 1.33 x U_s
Private communication from from D. Mitchell, Sandia Laboratories

Figure 11. P-x Diagram Showing Expected Progress of the Short-Duration Shock Wave Entering the Explosive and the Expected GTDD

Test results are summarized in Table 5. The threshold pressure is essentially constant for sample lengths from 0.78 to 2.54 mm. This is shown graphically in Figure 12. Also shown in Figure 12 are threshold pressures for 0.51- and 0.78-mm-long samples tested without timing measurements. These tests employed lucite (PMMA) witness blocks, impedance-matched to the HNS. A slightly larger value in threshold pressure seemed to be present with the shortest sample (0.51 mm); this supports the subsequent finding that the GTDD is about 0.6 mm. On those units that detonated the transit time, t_e (from shock input until shock output from the specimen), was then plotted as a function of pellet length in Figure 13. The inverse slope of this line agrees with the steady-state detonation velocity (6.86 mm/μs) of the HNS-SF. The excess transit time as shown graphically is 0.058 μs. On the basis that the entering shock, U_s, travels at 4.00 mm/μs (at 7.3 GPa) in unreacted HNS, then its intersection with the data line occurs at 0.56 mm (0.022 in.). This is the growth-to-detonation

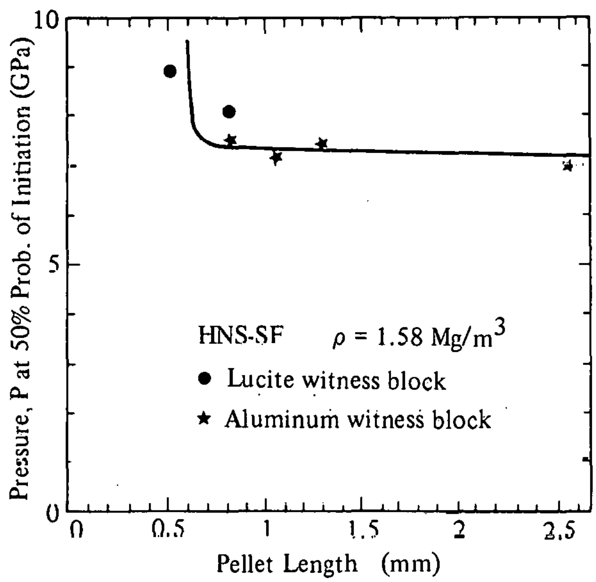

Figure 12. Threshold Pressure vs Sample Length

Table 5. Summary of HNS-SF Shock Sensitivity as a Function of Pellet Length (1.02-mm diameter x 0.076-mm thick flyer)

Pellet		Density	Test	No.	Initiation Threshold*				
Dia	Length	(Mg/m³)	Temp.(°C)	Tested	J_B(GA/m²)	v_f(mm/μs)	P(GPa)	τ(μs)	t_e(μs)
6.30	2.54	1.58 + 0.02	24	12	654 ± 16	2.25	7.0	0.035	0.428 ± 0.039
6.30	1.27	1.58 ± 0.02	24	12	702 ± 27	2.33	7.4	0.034	0.235 ± 0.009
6.30	1.04	1.58 ± 0.02	24	18	664 ± 55	2.29	7.2	0.035	0.224 ± 0.022
6.30	0.78	1.58 ± 0.02	24	17	720 ± 56	2.37	7.5	0.034	0.173 ± 0.016

*Initiation threshold is that input stimulus which produces a 50% probability of initiation to detonation. J_B is current density through the foil at burst; v_f is flyer velocity at impact with the explosive; P is the impact pressure; and τ is the pressure duration. The plus and minus values (J_B, t_e) are one standard deviation. The value t_e is the transit time through the explosive.

distance from these experiments. The graphical method is somewhat an oversimplification since it assumes that the steady shock velocity changes abruptly into steady detonation velocity; however, the GTDD is confirmed by the data in Figure 12. This GTDD is superimposed on the data in Figure 9, and illustrates the difference between the two sets of data.

It is concluded that the GTDD of HNS-SF from short-duration pulses is about one-half that of the HNS-I for which we have standard wedge test data. Thus, HNS-SF is a more desirable acceptor explosive because it will respond more promptly at lower pressure when struck by a thin flyer. Whether the reduction in GTDD is caused by the nature of the input stimulus, by some inherent difference in physical property such as number of initiation sites, or by some misinterpretation of the data from either test method is not evident.

Effect of Flyer Diameter[1, 2]

Sensitivity experiments were performed using two different flyer diameters, 1.02 and 1.57 mm, for impacting the explosive HNS-SF at a density of 1.60 Mg/m^3. The results are tabulated in Table 6.

The diameter effect is illustrated in the plot of Figure 14 in which threshold velocity was plotted against the reciprocal of flyer diameter. Based on this plot, one can make "infinite diameter" estimates based on the more easily obtained data at two small diameters. A straight line through the two data points intersected the datum point obtained by the Lawrence Livermore Laboratory[9] who used a large diameter flyer (25 mm). This data does not rule out the fact that there may be some flattening of the curve for large diameter flyers. The diameter effect is not unexpected if one assumes that wave divergence occurs and that some minimum diameter exists over which the stimulus must act.

Effect of Pulse Duration[2]

Previous experiments showed that, for a given pulse duration (τ), the pressure amplitude (P) of the input stimulus played a major role in shock initiation of high explosives. In this study, the effect of pulse duration on the shock initiation of HNS-SF was determined. Pulse duration was controlled by the flyer thickness which varied between 0.025 and 0.254 mm; the resulting τ varied from 0.010 to 0.137 μs, respectively. Sample density was 1.60 ± 0.01 Mg/m^3.

The shock-sensitivity data are summarized in Table 7 and in Figure 15. From Figure 15, it is noteworthy that as τ increases to values greater than 0.15 μs, the initiation criterion is one of nearly constant pressure ($\geq$3.6 GPa). Further, if one assumes the log P vs log τ relationship to be linear for τ between 0.01 and 0.10 μs, the initiation criterion, $P^n\tau$, is constant where $n = 2.4$.

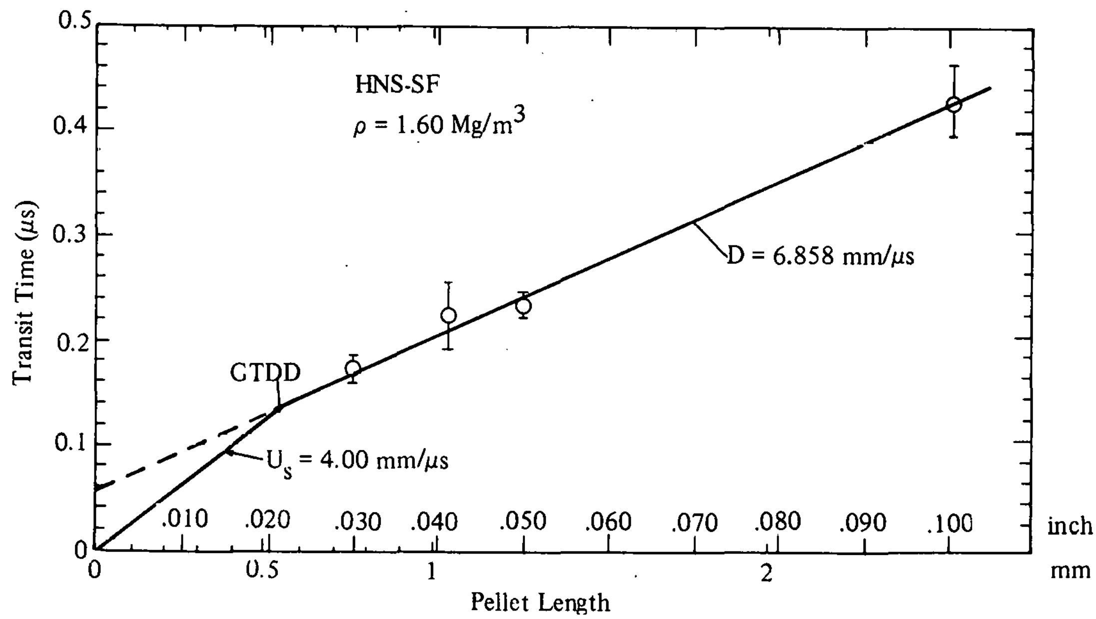

Figure 13. Growth to Detonation Distance Deduced From Transit Time Measurements

Table 6. Summary of HNS-SF Shock Sensitivity Data as a Function of Flyer Diameter (density 1.60 Mg/m³, flyer thickness 0.076 mm)

Flyer Diameter (mm)	Test Temp (°C)	Initiation Threshold* J_B(GA/m²)	v_f(mm/μs)	P(GPa)	τ(μs)
1.02	24	643±24	2.23±05	6.9	0.034
1.57	24	385±16	1.84±05	5.3	0.038

*Initiation threshold is that input stimulus which produces a 50% probability of initiation to detonation. J_B is current density through the foil at burst; v_f is flyer velocity at impact with the explosive; P is the impact pressure and τ is the pressure duration. The plus and minus values (J_B, v_f) are one standard deviation.

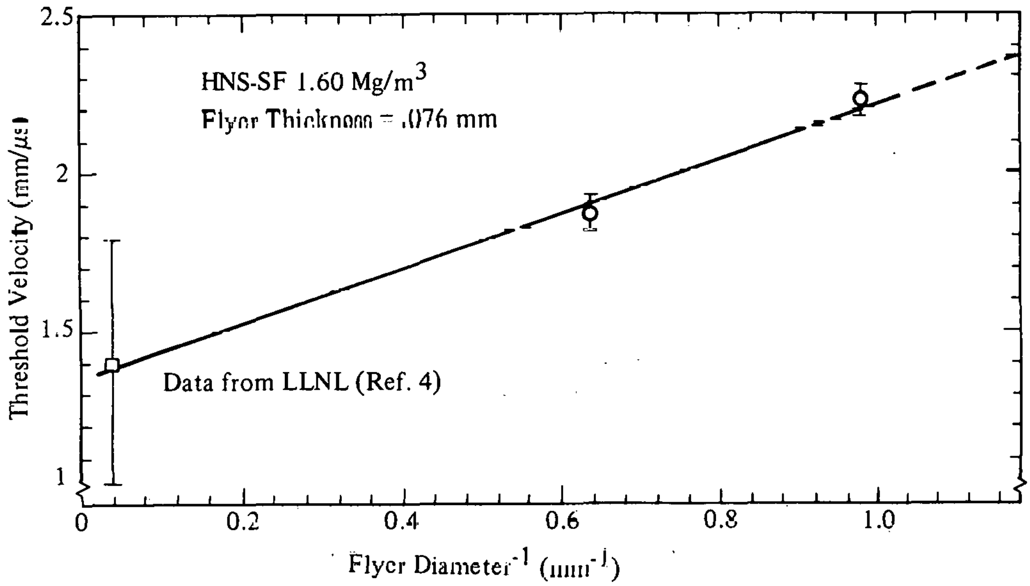

Figure 14. Effect of Flyer Diameter on Sensitivity

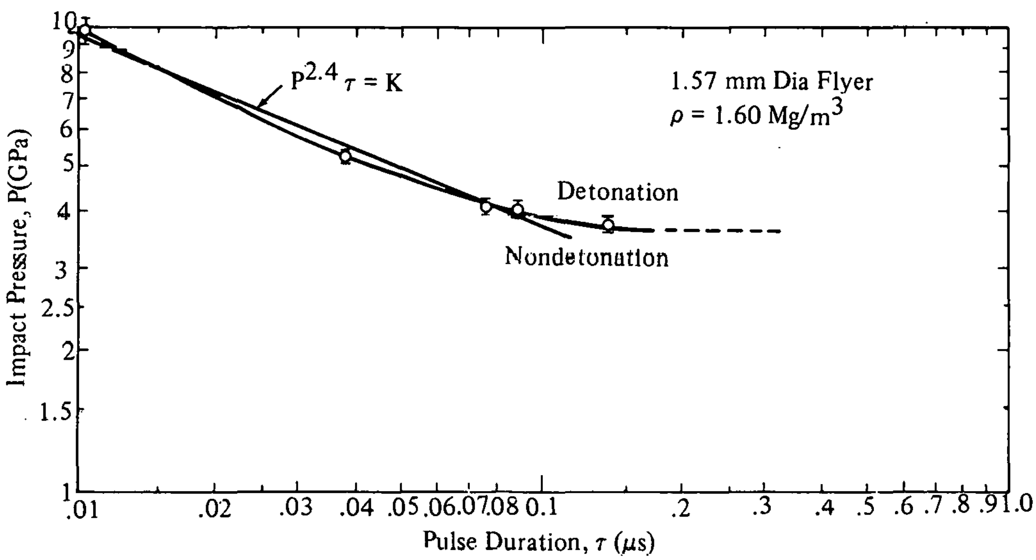

Figure 15. Effect of Pulse Duration on Initiation Sensitivity of HNS-SF

Table 7. Summary of HNS-SF Shock Sensitivity as a Function of Pulse Duration (test temperature 24°C, 1.57-mm diameter flyer)

Flyer Thickness		Initiation Threshold*			
(in.)	(mm)	J_B(GA/m^2)	v_f(mm/μs)	P(GPa)	τ(μs)
0.001	0.025	592±46**	2.84	9.8	0.011
0.003	0.076	385±16	1.84	5.3	0.038
0.0055	0.140	440±13	1.51	4.0	0.075
0.0065	0.165	506±16	1.53	4.1	0.097
0.010	0.254	665±20	1.46	3.8	0.137

*Initiation threshold is that input stimulus which produces a 50% probability of initiation to detonation. J_B is current density through the foil at burst; v_f is flyer velocity at impact with the explosive; P is the impact pressure; and τ is the pressure duration. The plus and minus values (J_B) are one standard deviation.

**This group used a foil thickness of 0.005 mm.

Comparing HNS-SF With LX-13 and HNAB[2]

Two additional explosive materials were evaluated to determine the effect of pulse duration on their initiation. The explosives were LX-13 and HNAB. LX-13 is an extrudable explosive containing 20% silicone rubber added to fine-particle PETN and has a density of 1.53 Mg/m^3. The HNAB contained large particles (a surface area of 0.031 m^2/g, average particle size of 82 μm) and was consolidated at a density of 1.60 Mg/m^3.

Test results are given in Table 8 and are shown graphically in Figure 16. Note from Figure 16 that HNAB and LX-13 illustrate the sensitivity "crossover" effect. This "crossover" in which rank-order of sensitivity changes with τ has been observed by many experimenters; it has been shown for PETN with fine and coarse particles;[10] also for RDX with fine and coarse particles;[11] also for PBXN-5 of two particle sizes.[12] A model explaining this phenomenon has been generated.[5]

Table 8. Summary of Shock Sensitivity Data of LX-13 and HNAB as a Function of Pulse Duration (flyer diameter 1.57 mm, test temperature 24°C)

Flyer Thickness		Initiation Threshold*			
(in.)	(mm)	J_B(GA/m^2)	v_f(mm/μs)	P(GPa)	τ(μs)
		LX-13 (Lot 216) ρ = 1.53 ±0.01 Mg/m^3			
0.001	0.025	693± 1	3.11	12.8	0.0097
0.003	0.076	414± 6	1.91	6.0	0.036
0.0055	0.140	520±17	1.67	5.0	0.070
0.010	0.254	890**	1.80	5.4	0.124
		HNAB (Lot 4063) ρ = 1.60 ±0.01 Mg/m^3			
0.001	0.025	>990	>4.90	>23.2	<0.0089
0.002	0.050	547±24	2.10	6.3	0.024
0.003	0.076	419±17	1.94	5.8	0.037
0.0055	0.140	434± 9	1.49	3.9	0.075
0.010	0.254	689±21	1.52	4.0	0.135

*Initiation threshold is that input stimulus which produces a 50% probability of initiation to detonation. J_B is current density through the foil at burst; v_f if flyer velocity at impact with the explosive; P is the impact pressure; and τ is the pressure duration. The plus and minus values (J_B) are one standard deviation.

**Insufficient data for standard deviation.

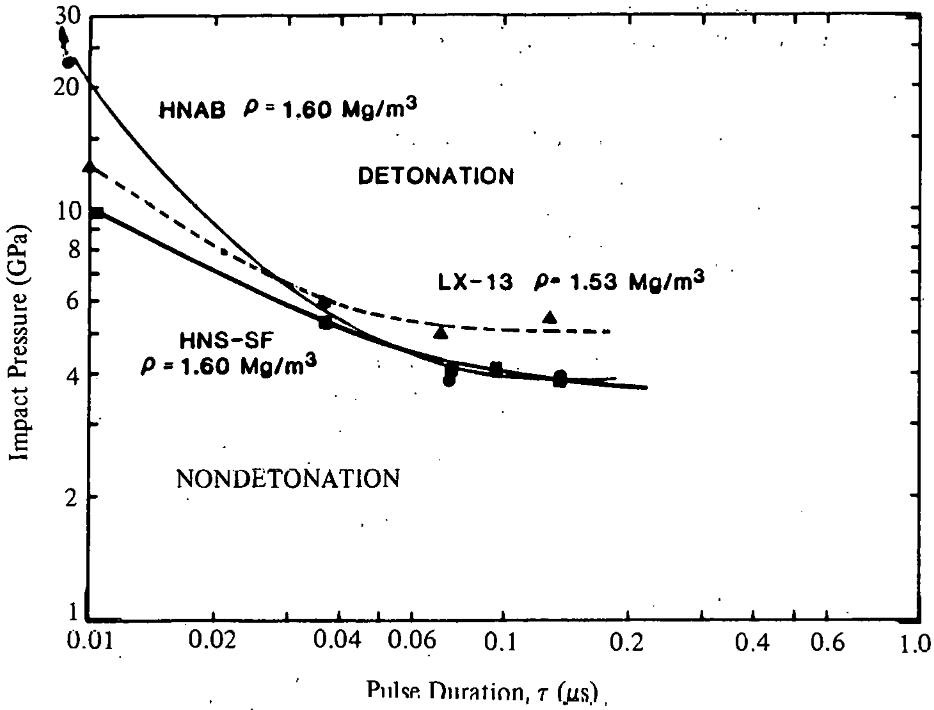

Figure 16. Shock Response of HNS-SF Compared to That of LX-13 and HNAB

It is noteworthy that the sensitivity of LX-13 becomes independent of pulse duration at about 5.0 GPa and that of HNAB at about 3.9 GPa compared to 3.6 GPa for HNS-SF.

The P-τ characterization is essential if one is to make the correct choice of explosive in component designs. The explosive chosen for short-pulse (0.01 to 0.02 μs) applications like minislapper dets is not necessarily best for thick flyer or through-bulkhead applications where pulse durations might be 0.1 to 0.3 μs.

Conclusions

Based on the test results reported here, it is concluded that:

- Powder morphology was one of the more significant factors which influenced the shock-initiation sensitivity of HNS; for 0.035μs duration pulses, there was a spread of nearly 50% in threshold pressure required to produce initiation, depending on the size of the particles of the explosives--smaller particles requiring less pressure. Not only was the small particle explosive more sensitive, it also was less variable in that it displayed a narrower band of pressure separating no-fire (.001 probability) from all-fire (.999 probability).
- The fact that lower density specimens, higher ambient temperature and the use of larger diameter flyers required a lesser stimulus to initiate HNS-SF is reasonable and can be explained, at least in part, by simple physics.
- The sample length must be great enough to allow sufficient time for growth-to-detonation to occur. HNS-SF appears to require a shorter growth-to-detonation distance than does HNS-I. The GTDD for HNS-SF is 0.56 mm at an impact pressure of 7.3 GPa.
- A complete P-τ characterization of each candidate explosive is essential if one is to chose the best explosive for a particular application. For example, a sensitivity crossover effect was noted for LX-13 and HNAB; for short duration pulses (like 0.01 μs) LX-13 was more sensitive; for longer pulses (like 0.1μs) HNAB was more sensitive.
- Future work should include the evaluation of other shock-sensitive materials such as pyrotechnics or propellants.

References

[1]E. E. Kilmer, "*Heat-Resistant Explosives for Space Applications*," Journal of Spacecraft, 5(10): October 1968.

[2]A. C. Schwarz, *Application of Hexanitrostilbene (HNS) in Explosive Components*, SC-RR-710673 (Albuquerque: Sandia Laboratories, May 1972).

[3]H. E. Anderson, *STAT/LIB*, SAND74-0225 (Albuquerque: Sandia Laboratories, October 1974)

[4]A. C. Schwarz, *"A New Technique for Determining the Shock Initiation Sensitivity of Explosives,"* Proceedings of the Conference on the Standardization of Safety and Performance Tests of Energetic Materials, U. S. Army Armament Research and Development Command, Dover, NJ, September, 1977.

[5]D. B. Hayes and D. E. Mitchell, *"A Constitutive Equation for the Shock Response of Porous Hexanitrostilbene (HNS) Explosive,"* presented at HDP Symposium, Paris, France, August 1978.

[6]J. Roth, *"Shock Sensitivity and Shock Hugoniots of High Density Granular Explosives,"* Proceedings of the Fifth Symposium on Detonation ACR-184, Pasadena, CA, August 1970, published by ONR, Dept of Navy.

[7]J. B. Ramsay and A. Popolato, *"Analysis of Shock Wave and Initiation Data for Solid Explosives,"* Proceedings of Fourth Symposium on Detonation, ONR ACR-126, October 1965.

[8]D. E. Mitchell, *C-4 Energy Transfer System Experiments and Performance Calculations*, SAND77-2029 (Albuquerque: Sandia Laboratories, March, 1978).

[9]R. Jackson, formerly at Lawrence Livermore Laboratory, Private Communication.

[10]A. C. Schwarz, *Feasibility Study of a Fail-Safe Through Bulkhead Initiator*, SAND78-1696 (Albuquerque: Sandia Laboratories, March, 1980).

[11]Y. deLongueville, C. Fauquignon, and H. Moulard, *"Initiation of Several Condensed Explosives by a Given Duration Shock Wave,"* Sixth Symposium on Detonation, ACR-211, Office of Naval Research, August, 1976.

[12]R. H. Stressau and J. E. Kennedy, *"Critical Conditions for Shock Initiation of Detonation in Real Systems,"* Sixth Symposium on Detonation, ACR-221, Office of Naval Research, August 1976.

Appendix

Hugoniot Data Used for Computations

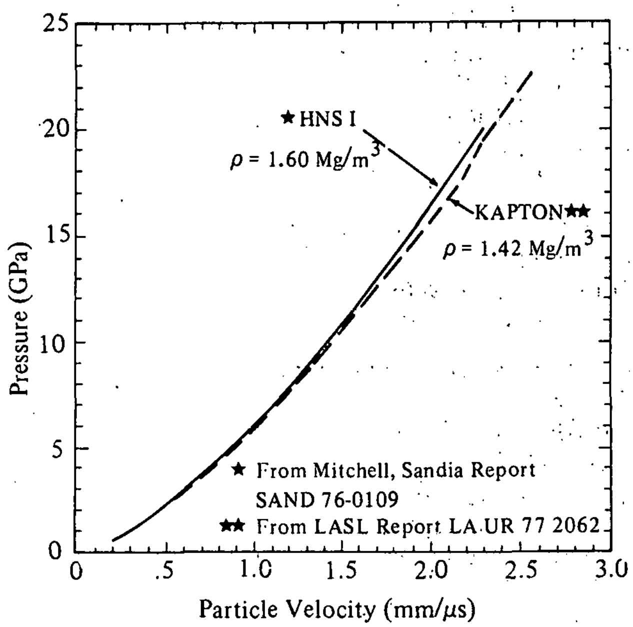

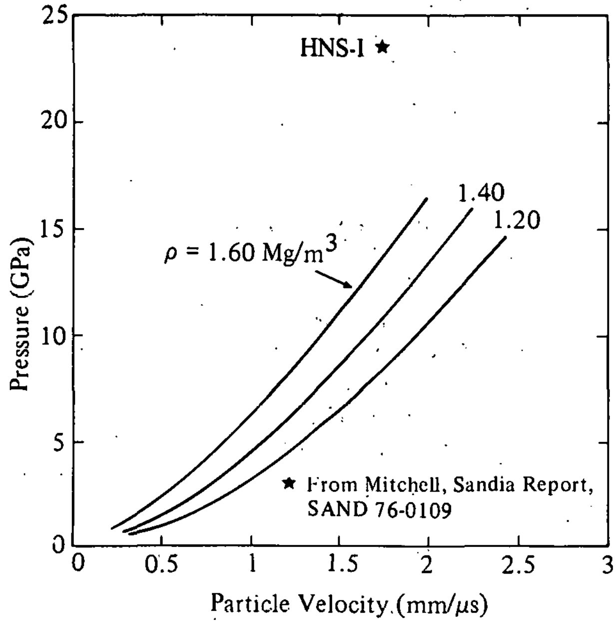

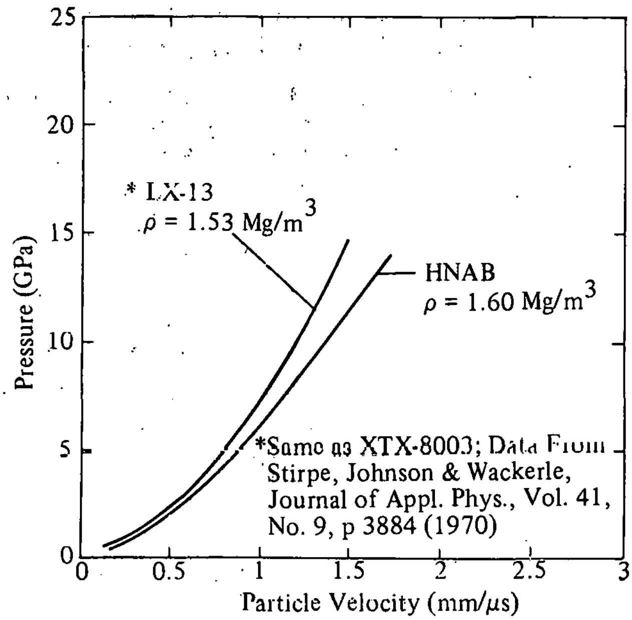

DISTRIBUTION:

Naval Surface Weapon Center (2)
White Oak Laboratory
Silver Spring, MD 20910
Attn: E. E. Kilmer
F. L. Menz

Ensign Bickford Co. (2)
660 Hopmeadow Street
Simsbury, CT 06070
Attn: B. Boggs
P. Murphy

Explosive Technology (2)
P. O. Box KK
Fairfield, CA 94533
Attn: G. B. Huber
M. C. Anderson

Lawrence Livermore Laboratory (5)
P. O. Box 808
Livermore, CA 94550
Attn: N. Schneider (L-368)
Frank Walker (L-50)
Brigitta Dobratz (L-326)
Ken Scribner (L-324)
R. C. Weingart (L-368)

Jet Research Center, Inc.
P. O. Box 246
Arlington, TX 76010

R. Stresau Laboratory
Star Route
Spooner, WI 54801
Attn: R. Stresau

Teledyne McCormick Selph
P. O. Box 6
Hollister, CA 95023
Attn: H. Anderson

McDonnell Douglas Corp.
P. O. Box 516
St. Louis, MO 63166
Attn: M. L. Schimmel

Dept. of Army
ARRADCOM
Dover, NJ 07801
Attn: W. Voreck, Explosives
Trains Section

Franklin Research Center (2)
Philadelphia, PA 19103
Attn: E. E. Hannum
P. F. Mohrback

NASA - Langley Research Center
Langley Station
Hampton, VA 23365
Attn: L. J. Bement, 246E

Unidynamics/Phoenix, Inc. (3)
P. O. Box 2990
Phoenix, AZ 85062
Attn: C. Simpson
R. Smith
J. Fronaberger

Reynolds Industries, Inc. (2)
P. O. Box P850
Marina Del Rey, CA 90291
Attn: G. E. Sheridan
B. MacDonald

Lockheed Missiles and Space Co.
P. O. Box 504
Sunnyvale, CA 94088
Attn: R. Guay, SPL-30

Los Alamos Scientific Laboratory (4)
P. O. Box 1663
Los Alamos, NM 87545
Attn: G. Seay, WX-7
W. Meyers, WX-5
T. Larson, WX-2
R. Rogers, WX-2

National Aeronautics and Space Administration
Johnson Space Center
Houston, TX 77058
Attn: T. J. Graves

Monsanto Research Corporation (6)
Mound Facility
Miamisburg, OH 45342
Attn: H. L. Turner
J. R. Brinkman
R. J. DeSando
M. A. Witzerman
W. L. Schurman
T. K. Ferguson

Mason & Hanger, Silas Mason Co. (2)
P. O. Box 30020
Amarillo, TX 79177
Attn: C. D. Alley
R. J. Slape

Systems, Science & Software (2)
P. O. Box 1620
La Jolla, CA 92038
Attn: E. Day
R. Wilson

DISTRIBUTION: (cont)

Space Ordnance Systems, Inc. (2)
25977 Sand Canyon Road
Canyon Country, CA 91351
Attn: R. Ritchie
J. Neeley

Hi-Shear Corporation (2)
2830 West Lomita Blvd.
Torrance, CA 90505
Attn: G. Leiter
H. Haque

Denver Research Institute
University of Denver
Denver, CO 80208
Attn: R. M. Blunt

IIT Research Institute
10 West 35th Street
Chicago, IL 60616
Attn: A. J. Tulis

Roberts Research Lab
20802 South Normandy Avenue
Torrance, CA 90502
Attn: L. Roberts

Commanding Officer
Air Force Technical Applications Center
Washington, DC 20333
Attn: TD-6

Air Force Weapons Laboratory
Technical Library
Kirtland AFB, NM 87117
Attn: E. L. Bowman

Atomic Weapons Research Establishment
Adlermaston, Reading RG7 4PR
Berkshire, England
Attn: J. Kirkham

Martin Marietta Aerospace
P. O. Box 5837
Orlando, FL 32805
Attn: E. Storma, 136

Institut Für Chemie Der Treib-Und
Explosivstoffe
7507 Pfinztal-Berghausen Bei
Karlsruhe
Postfach 40 Germany
Attn: F. Volk

400 C. Winter
1200 L. D. Smith
1230 W. L. Stevens
Attn: S. D. Spray
1415 J. T. Hillman
1533 F. H. Mathews
1700 W. C. Myre
2000 E. D. Reed
2167 J. H. Stichman
2500 J. C. Crawford
2510 D. H. Anderson
2513 J. E. Kennedy
2513 P. L. Stanton
2514 B. H. VanDomelen
2515 P. D. Wilcox
2515 A. C. Schwarz (10)
2516 W. G. Perkins
Attn: R. G. Jungst
2526 J. J. Marron
3440 L. M. Jercinovic
4300 R. L. Peurifoy, Jr.
4330 E. E. Ives
4360 J. A. Hood
5131 B. Morosin
5510 D. B. Hayes
5534 J. R. Asay
5600 D. B. Shuster
8110 J. Barham
8162 A. S. Rivenes
8300 B. F. Murphey
8214 P. A. Childers
3141 L. J. Erickson (5)
3151 W. L. Garner (3)
For: DOE/TIC (Unlimited Release)
DOE/TIC (25)
(J. Hernandez, 3154-4)

Org.	Bldg.	Name	Rec'd by *	Org.	Bldg.	Name	Rec'd by